Electrochemical Formation of Self-Organized Nanotubular Oxide Layers on Ti13Zr13Nb Alloy for Biomedical Applications

A. Smołka[a,*], K. Rodak[b], G. Dercz[a], K. Dudek[a] and B. Łosiewicz[a,*]

[a]Institute of Materials Science, Silesian Interdisciplinary Centre for Education and Research
University of Silesia, 75 Pułku Piechoty 1A, 41-500 Chorzów, Poland
[b]Faculty of Chemistry, Silesian University of Technology, B. Krzywoustego 6, 44-100 Gliwice, Poland
[c]Faculty of Materials Engineering and Metallurgy, Z. Krasińskiego 8, 40-019 Katowice, Poland

In this work, the anodic formation of self-organized nanotubular oxide layers on Ti13Zr13Nb implant alloy was presented. Anodic oxidation was carried out at room temperature in [1 M] $(NH_4)_2SO_4$ solution with 1 wt% content of NH_4F. The voltage and time of anodization was 20 V for 120 min, respectively. Under proposed conditions, the best arrangement of nanopores was observed. The physical and chemical properties of the anodized surface of the Ti13Zr13Nb alloy were characterized using grazing incidence X-ray diffraction, scanning transmission electron microscopy, and atomic force microscopy. It was found that diameter of nanopores varied from 10 to 32 nm. Mechanism of the fabrication of the unique 3D tube-shaped nanostructure of TiO_2 on the surface of the Ti13Zr13Nb alloy by electrochemical anodization, has been discussed.

1. Introduction

Implantable materials make critical contributions to modern medicine. The human body presents a very challenging environment for materials engineers because of the need for implants that are higly corrosion resistant, biocompatible, and able to bond to bone during osseointegration [1–5].

Metallic biomaterials have been in the past, and will continue to be in the future, used in implants spanning all areas of the use in the human body like orthopedic, spinal, dental, cardiovascular, neural, urological, and other applications [1]. Metallic biomaterials will remain central to such medical applications due to their unique properties compared to those of other groups of materials.

An active area of research in metallic biomaterials involves new titanium alloys, especially β-structure alloys which exhibit low elastic modulus, ability to utilize large oxygen additions without brittle failure, lower notch sensitivity in fatigue, and are able to work harden and cold from shapes. Unfortunately, in most used in medicine titanium alloys, the toxic elements, e.g. Ni, V or Al, are present and their release in the human body can lead to the Alzheimer disease, neuropathy, metalosis or allergic reactions. Therefore, in recent years more biocompatible elements like Ta, Nb, Zr, Sn or Pd, which for example play a role of β structure stabilizer in titanium, were started to be applied. To eliminate these health problems, an alternative, multifunctional and biocom-

patible titanium alloy, Ti13Zr13Nb, has been developed, which is based only on non-toxic elements. This alloy exhibits optimal mechanical and plastic properties as well as high corrosion resistance and biocompatibility resulting from the spontaneous formation of the passive oxide layer TiO_2 and small amount of Nb_2O_5 and ZrO_2 on the surface [1–3, 6].

Recently, anodizing is a developed method of the surface modification of titanium and its alloys. Anodizing process carried out under specified conditions (voltage, electrolyte type and pH, time path) results in formation of nanostructures on the surface [4, 5]. It has been reported that the presence of nanotubes on the surface of titanium and its alloys improves the adhesion and proliferation of cells for medical application [7]. The structure of nanotubes allow to use them in targeted drug delivery systems or to encapsulate proteins and enzymes.

The aim of the present study is to investigate the self-organized formation of nanotubular oxide layers by anodizing of the Ti13Zr13Nb implant alloy in the electrolyte based on ammonia sulfate with fluorine-ion addition.

2. Experimental

The tested samples of the Ti13Zr13Nb alloy with dimension of $7 \times 4 \times 0.8$ mm^3 were cut from flat bars. Composition of the Ti13Zr13Nb alloy is given in wt%. The samples were ground with 600# grit silicon carbide paper, sonicated for 20 min using nanopure water (Milli-Q, 18.2 MΩ cm^2, < 2 ppb total organic carbon), and then electropolished. The bath composition and time used for electropolishing procedure are described in Ref. [7]. Electropolishing was carried out at a current density of 1.4 A cm^{-2} for 4.4 min. Next, the samples were cleaned in ultrasonic bath in nanopure water. Anodic oxidation

*corresponding author; e-mail: agnieszka.smolka@us.edu.pl, bozena.losiewicz@us.edu.pl

was performed at room temperature in [1 M] $(NH_4)_2SO_4$ solution with 1 wt% content of NH_4F. Value of pH solution was 6.3. The time and voltage of anodization was 120 min and 20 V, respectively. The two-electrode electrochemical cell was used with a working electrode (anode) made of the Ti13Zr13Nb alloy and a platinum foil (cathode) as a counter electrode. The distance between cathode and anode was 25 mm. The sample under investigation was placed inside a self-designed Teflon holder which contained O-ring. The exposed surface area of the electrode was 0.64 cm^2. Anodization process was carried out using a MAG-5N galvanizing aggregate.

The morphology and structure of the formed nanotubular oxide layers was examined using a HITACHI HD-2300A scanning transmission electron microscopy (STEM) and the grazing incidence X-ray diffraction (GIXD) on the X'Pert Philips PW 3040/60 diffractometer operating at 30 mA and 40 kV, which was equipped with a vertical goniometer and an Eulerian cradle, respectively. The wavelength of radiation (λ Cu K_α) was 1.54178 Å. The GIXD patterns were registered in the 2θ range from 10 to 50° with a 0.05° step for the incident 0.25°, 0.50°, 1.00° angle. The chemical composition of the alloy was analyzed by energy dispersive X-ray spectroscopy (EDS). The QScope^{TM} 250 atomic force microscope (AFM) (Quesant Instrument Corporation, Agoura Hills, CA) integrated into the Hysitron TI 950 TriboIndenter, was used to study the topography and roughness of the surface.

3. Results and discussion

Figure 1 shows STEM images of the surface morphology of the Ti13Zr13Nb alloy after anodization carried out under optimal electrochemical conditions at 20 V for 120 min in [1 M] $(NH_4)_2SO_4$ solution with the content of 1 wt% NH_4F. One can see in the top view of TiO_2 nanotube layer formed on the Ti13Zr13Nb alloy (Fig. 1a) that the addition of NH_4F influences the dissolution of parts of the oxide layer in which nanotubular structures are formed. Typical, broad cracks of the TiO_2 layer are visible at low magnification [1, 9]. Figure 1b presents the characteristic image at high magnification of the top view of nanotubes formed by anodization on Ti13Zr13Nb alloy. A uniform distribution of the single-walled TiO_2 nanotubes is visible. A chosen area for estimation of the nanotube diameter shows that by anodizing of the Ti13Zr13Nb alloy under proposed conditions, the single-walled TiO_2 nanoutbes with internal diameter in the range from 12 to 32 nm, can be formed (Fig. 1c).

EDS analysis revealed the presence of peaks originating from the substrate, such as Ti, Zr and Nb (Fig. 2). The obtained results confirm the chemical composition of the alloy under investigation. The oxygen peak in the spectrum indicates that the oxide layer on the Ti13Zr13Nb alloy surface is present.

Figure 3 shows the GIXD pattern of the Ti13Zr13Nb alloy after anodization at 20 V for 120 min. Presence of titanium oxide (TiO_2 rutile, ICDD PDF 00-034-0180) was confirmed using the GIXD technique. Additionally,
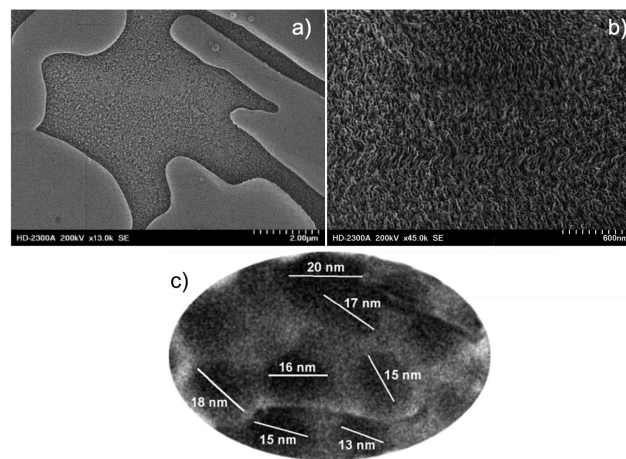

Fig. 1. STEM image of the surface morphology of TiO_2 nanotube layer formed on the Ti13Zr13Nb alloy: (a) top view at high magnification, (b) top view at low magnification, and (c) chosen area for estimation of the nanotube diameter.
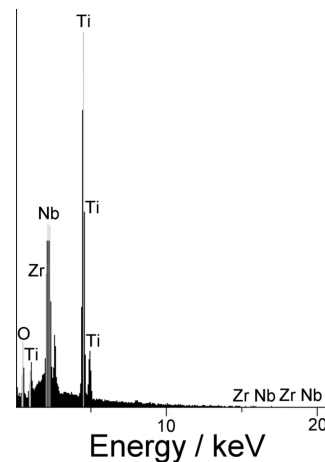

Fig. 2. EDS analysis of the Ti13Zr13Nb alloy after anodization at 20 V for 120 min.

the phase analysis revealed the presence of two phases from substrate: α-Ti (ICDD PDF 00-044-1294) and β-Ti (ICDD PDF 01-089-3726).

A typical AFM image of the surface of the Ti13Zr13Nb alloy before anodization in 2D (Fig. 4a) and 3D (Fig. 4b) view is presented. The determined mean roughness index, R_a, of the tested surface equals 4.3 nm, indicating very smooth surface morphology. After anodization of the Ti13Zr13Nb alloy in the appropriate conditions, the surface development has changed (Fig. 5a and b). The surface roughness significantly increased and $R_a = 92.9$ nm. The obtained results point that anodizing of the tested alloy caused the increase in surface roughness more than 20 times as compared to the Ti13Zr13Nb alloy before formation of TiO_2 nanotubes.

Based on the obtained results, the mechanism of TiO_2 nanotubes formation on the Ti13Zr13Nb alloy in the electrolyte based on ammonia sulfate with fluorine-ion addi-
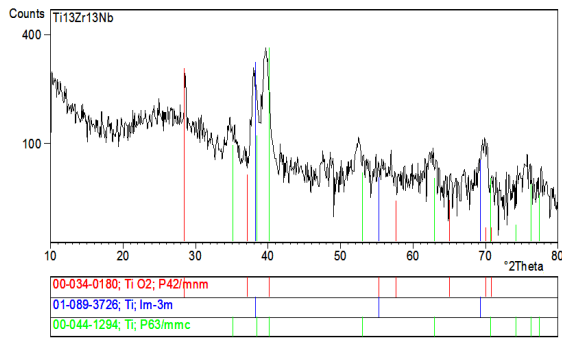
Fig. 3. GIXD pattern of the Ti13Zr13Nb alloy after anodization at a 20 V for 120 min.
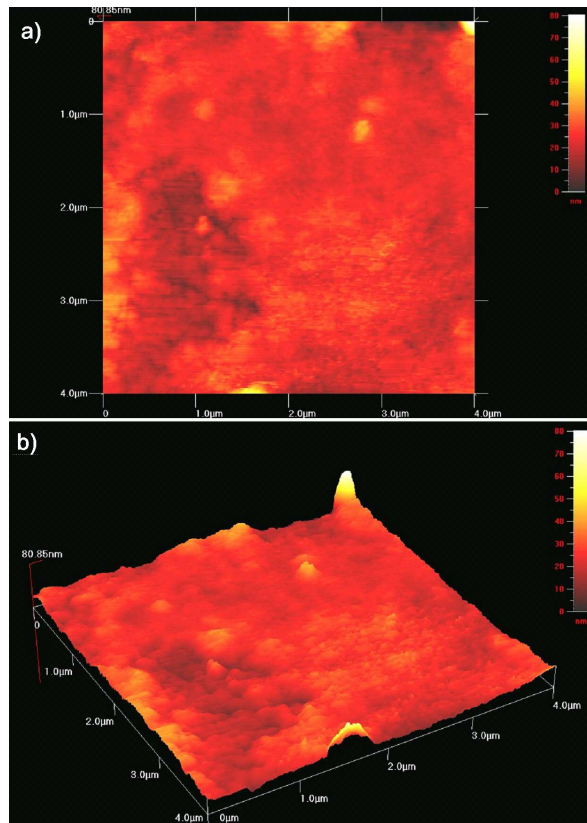

Fig. 4. The AFM image of the surface of the Ti13Zr13Nb alloy before anodization: (a) 2D, and (b) 3D view.

tion, was presented schematically in Fig. 6. In accordance with the literature data concerning formation of self-organized nanotubular oxide layer on Ti [1, 9, 10], in case of the Ti13Zr13Nb alloy anodization also three simultaneous processes have to be considered. This is the field assisted oxidation of Ti metal to form TiO_2, the field assisted dissolution of Ti metal ions in the electrolyte, and the chemical dissolution of Ti and TiO_2 due to etching by fluorine ions, which is enhanced by the presence of H^+ ions. It should be noted that self-organized
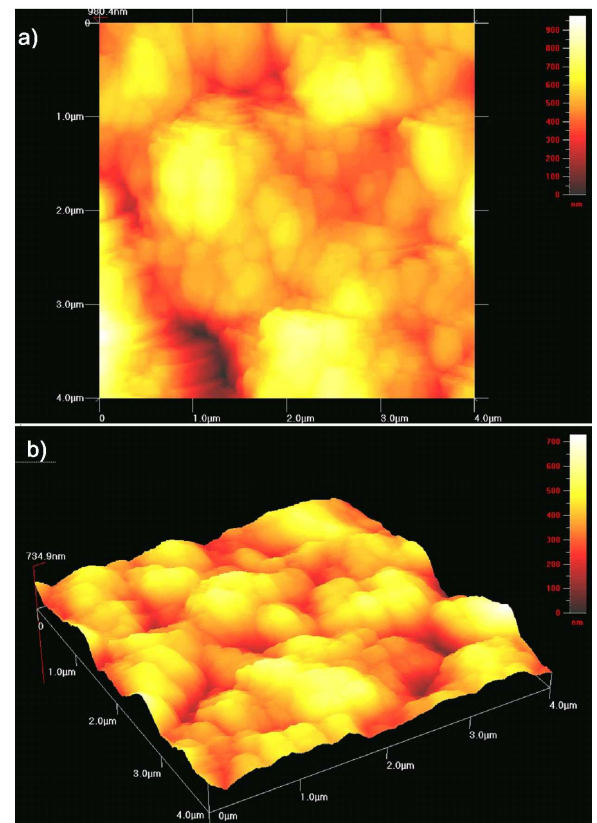

Fig. 5. The AFM image of the Ti13Zr13Nb alloy after anodization at a 20 V for 120 min: (a) 2D, and (b) 3D view.
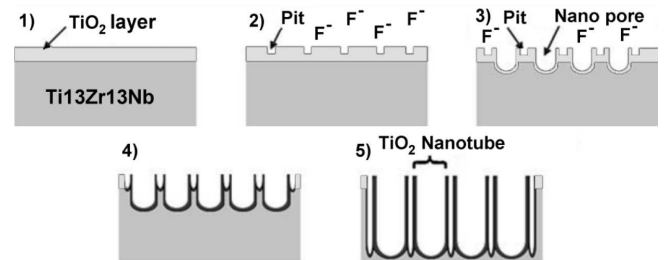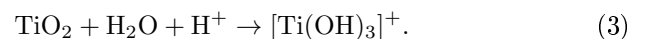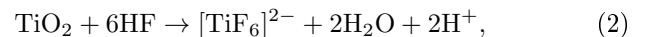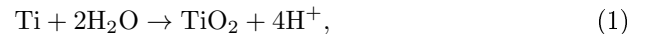

Fig. 6. Scheme of the TiO_2 nanotube formation on the surface of the Ti13Zr13Nb alloy, inspired by Fig. 1 from Ref. [9].

TiO_2 nanotubes are not formed on the pure surface of the Ti13Zr13Nb alloy but on the thin TiO_2 oxide layer naturally present on the alloy surface. Therefore, the mechanism of TiO_2 nanotubes formation is related to the kinetics of two processes: oxidation (1) and dissolution (2), (3):

$$Ti + 2H_2O \rightarrow TiO_2 + 4H^+, \tag{1}$$

$$TiO_2 + 6HF \rightarrow [TiF_6]^{2-} + 2H_2O + 2H^+, \tag{2}$$

$$TiO_2 + H_2O + H^+ \rightarrow [Ti(OH)_3]^+. \tag{3}$$

The phenomena of anodic formation of nanotubular oxide layers on pure Zr and Nb was also observed in the literature [1, 9, 10], however, in case of the Ti13Zr13Nb alloy, the oxide layer is revealed by XRD as rutile. In

Fig. 3 one can also observe amorphous halo which can be related to the presence of other amorphous oxides on the alloy surface, undetectable by XRD [8]. For a description of the formation of TiO_2 nanotubes by anodization process displayed in Fig. 6, the anodization mechanism of creating the nanotube structure is divided into five steps: 1 — before anodization, a nanoscale TiO_2 passive layer is present on the Ti13Zr13Nb alloy surface, 2 — when constant voltage is applied, a pit is formed on the TiO_2 layer, 3 — as anodization time increases, the pit grows longer and larger, and then it becomes a nanopore, 4 — nanopores and small pits undergo continuous barrier layer formation, and 5 — after specific anodization time, completely developed nanotubes are formed on the Ti13Zr13Nb surface.
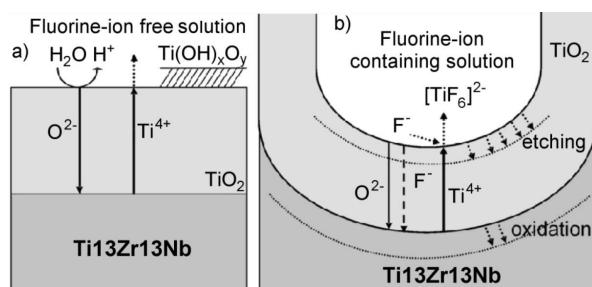

Fig. 7. Anodization scheme of the Ti13Zr13Nb alloy: (a) in the absence, and (b) in the presence, of fluorine anions, inspired by Fig. 1 from Ref. [10].

The nanotubular structure formation depends on the anodization conditions and especially on the concentration of fluorine ions in the solution. It is well known that with the increase in the applied voltage, larger diameter nanotubes can be formed. This aspect of diameter manipulation using applied voltage was widely discussed in Refs. [9] and [10]. Anodization scheme of the Ti13Zr13Nb alloy in the absence and in the presence of fluorine anions, is shown in Figs. 7a and b, respectively. Reaction (1) describes the Ti oxide growth on the anodized surface of the Ti13Zr13Nb alloy in the absence of fluorine anions in solution (Fig. 7a). Oxidized Ti species react with O^{2-} ions coming from dissolution of water particle and form the oxide layer. Next, the oxide growth takes place and this process is controlled by field-aided ion transport of O^{2-} and Ti^{4+} through the growing oxide. This layer is typically loose and porous.

In the presence of fluorine ions (Fig. 7b), according to reaction (2), water-soluble TiF_6^{2-} complexes are formed. Due to the small ionic radius, F^- ions can enter the growing TiO_2 lattice and to be transported through the oxide by the applied field. According to reaction (3), the complex formation ability leads to a permanent chemical dissolution of formed titanium dioxide and prevents $Ti(OH)_xO_y$ precipitation as Ti^{4+} ions arriving at the oxide solution interface can be solvatized to TiF_6^{2-} before reacting to a precipitate $Ti(OH)_xO_y$ layer [10].

4. Conclusions

The obtained results of EDS, STEM, GIXD and AFM studies confirmed the possibility of electrochemical formation of self-organized nanotubular oxide layers on Ti13Zr13Nb implant alloy under proposed conditions. The result of the anodization carried out in [1 M] $(NH_4)_2SO_4$ solution with 1 wt% content of NH_4F at room temperature at 20 V for 120 min, was formation of TiO_2 (rutile) nanotubes. The diameter that can be obtained ranged from 10 to 32 nm. The mechanism of the TiO_2 nanotubes formation is based on the field assisted oxidation of Ti metal to form TiO_2, the field assisted dissolution of Ti metal ions in the electrolyte, and the chemical dissolution of Ti and TiO_2 due to etching by fluorine ions, which is enhanced by the presence of H^+. The obtained results suggest that the proposed method of surface modification is promising for better osseointegration of the Ti13Zr13Nb implant alloy.

References

[1] *Comprehensive Biomaterials*, Eds. P. Ducheyne, K.E. Healy, D.W. Hutmacher, D.W. Grainger, C.J. Kirkpatrick, Elsevier Sci., Amsterdam 2011.

[2] W. Yu, J. Qiu, L. Xu, *Biomed. Mater.* **4**, 065012 (2009).

[3] Z. Xu, Q. Li, *J. Mater. Sci. Technol.* **28**, 865 (2012).

[4] S. Bai, D. Ding, C. Ning, R. Qin, L. Huang, *Electrochem. Commun.* **12**, 152 (2010).

[5] C.E.B. Marino, L.H. Mascaro, *J. Electroanal. Chem.* **568**, 115 (2004).

[6] B. Łosiewicz, G. Dercz, M. Szklarska, W. Simka, M. Łężniak, A. Krząkała, A. Swinarew, *Solid State Phenom.* **203-204**, 212 (2013).

[7] J.R. Davies, in: *Handbook of Materials for Medical Devices*, Ed. J.R. Davies, ASM International, Ann Arbor 2003, p. 193.

[8] W. Simka, M. Mosiałek, G. Nawrat, P. Nowak, J. Żak, J. Szade, A. Winiarski, A. Maciej, L. Szyk-Warszyńska, *Surf. Coat. Technol.* **213**, 239 (2012).

[9] K.S. Brammer, S. Oh, C.J. Frandsen, S. Jin, in: *Biomaterials Science and Engineering*, Ed. R. Pignatello, InTech, Rijeka 2011.

[10] J.M. Macak, H. Tsuchiya, A. Ghicov, K. Yasuda, R. Hahn, S. Bauer, P. Schmuki, *Curr. Opin. Solid State Mater. Sci.* **11**, 3 (2007).